

# Polymer Chemistry

Accepted Manuscript



This is an *Accepted Manuscript*, which has been through the Royal Society of Chemistry peer review process and has been accepted for publication.

*Accepted Manuscripts* are published online shortly after acceptance, before technical editing, formatting and proof reading. Using this free service, authors can make their results available to the community, in citable form, before we publish the edited article. We will replace this *Accepted Manuscript* with the edited and formatted *Advance Article* as soon as it is available.

You can find more information about *Accepted Manuscripts* in the [Information for Authors](#).

Please note that technical editing may introduce minor changes to the text and/or graphics, which may alter content. The journal's standard [Terms & Conditions](#) and the [Ethical guidelines](#) still apply. In no event shall the Royal Society of Chemistry be held responsible for any errors or omissions in this *Accepted Manuscript* or any consequences arising from the use of any information it contains.

Cite this: DOI: 10.1039/c0xx00000x

www.rsc.org/xxxxxx

ARTICLE TYPE

## A green route to water-soluble polyaniline for photothermal therapy catalyzed by iron phosphate peroxidase mimic

Leilei Li,<sup>a</sup> Kaixuan Liang,<sup>a</sup> Zhentao Hua,<sup>a</sup> Min Zou,<sup>b</sup> Kezheng Chen<sup>\*a</sup> and Wei Wang<sup>\*a</sup>*Received (in XXX, XXX) Xth XXXXXXXXX 20XX, Accepted Xth XXXXXXXXX 20XX*

DOI: 10.1039/b000000x

A green route to water-soluble polyaniline (PANI) using iron phosphates (FePOs) peroxidase mimic as catalyst and H<sub>2</sub>O<sub>2</sub> as oxidant is presented. Polystyrene sulfonate (PSS) is used as template to synthesize conductive PANI-PSS complex. PANI samples were characterized by UV-Vis spectroscopy, FT-IR spectroscopy and bulk conductivity measurement. Results indicated that the conductivity of the PANI catalyzed by FePOs peroxidase mimic greatly depends on the pH, temperature and molar ratio of H<sub>2</sub>O<sub>2</sub> and aniline. Superior to natural horseradish peroxidase, the prepared FePOs demonstrated robust catalytic ability and could catalyze the formation of PANI-PSS at much lower pH values of 1.5~2.6. Photothermal effect of the FePOs catalyzed PANI samples was investigated and a high light-to-heat conversion efficiency of 39.6% was obtained for the sample with a conductivity of 2.576×10<sup>-3</sup> S/cm. Excellent biocompatibility and remarkable anti-tumor effect were observed for the prepared PANI with human cervical cancer (HeLa) cells as a cell model.

### Introduction

Photothermal therapy (PTT) method, which employs photothermal agents for achieving photothermal damage of tumors, has been explored in the past decade. These photothermal agents are capable of converting light energy into heat with different conversion efficiency, making the temperature increase above the thermal damage threshold to destruct the cancer cells. Ideal photothermal agents should possess strong absorbance in near-infrared region (NIR), low toxicity and high light-to-heat converting efficiency.<sup>1,2</sup> Currently, available PTT agents mainly comprise metal nanoparticles (Ag,<sup>3-5</sup> Au,<sup>6-8</sup> Pd,<sup>9-10</sup> Ge<sup>11</sup>), carbon based materials<sup>12</sup> and semiconductor nanoparticles.<sup>13</sup> Ag/Au/Pd nanoparticles, exhibiting distinct surface-plasmon-resonance (SPR) property, possess intense absorption in NIR region and relatively high photothermal conversion efficiency. Especially, the conversion efficiency of Au nanorods, prepared by Xiao et al,<sup>1</sup> is amazingly as high as 98.6%. However, gold nanostructures have low photostability in that their NIR absorbance peak would diminish due to the melting effect after being irradiated for a long period.<sup>14,15</sup> In addition, the high expense limited the wide use of noble metal nanoparticles. Also these materials are inorganic, which usually are not biodegradable and may remain inside of human body for long time after systemic administration. Alternatively, polymeric materials<sup>16-19</sup> geared towards application in PTT have been attracting attention. Among these reported compounds, polyaniline (PANI) is the firstly reported<sup>20</sup> and perhaps one of the most useful conducting polymers due to its low cost, good conductivity and high absorbance in NIR.<sup>16,20,21</sup> Moreover, PANI is non-cytotoxic and has been used as an electroactive material for studying cellular proliferation.<sup>22</sup>

Although PANI has such properties, its polymerization usually depends on chemical and electrochemical methods. Both the methods whether are environmentally hazardous or the synthesized product isn't water-soluble. These disadvantages seriously affect the processability and application of PANI. So there is increasing interest in environmentally friendly routes to the synthesis of conducting water-soluble PANI. Enzyme-catalyzed polymerization of polymers are attracting great interest since enzymatic approach can overcome many strong drawbacks in traditional chemical process. First of all, enzymatic protocol involves eco-friendly oxidants such as H<sub>2</sub>O<sub>2</sub> and molecular oxygen rather than ammonium peroxydisulfate, which is an environmentally incompatible oxidant, used in traditional process. Secondly, the use of ammonium peroxydisulfate results in formation of a large amount of by-products, whereas in the case of H<sub>2</sub>O<sub>2</sub> the formation of H<sub>2</sub>O as the only reduction product greatly simplifies post-treatments and recycling. Thirdly, enzymatic approach can offer a higher degree of control over the kinetics of the reaction. Moreover, enzyme-catalyzed conductive polymers are superior to those synthesized by traditional methods in that they are water-soluble and hence desirable for practical applications. Enzymatically-produced conducting water-soluble PANI has the opportunity to be at the forefront of converting the production methods for novel and evolving polymeric materials to more sustainable and environmentally friendly routes. The commonly used natural enzymes, such as horseradish peroxidase (HRP),<sup>23</sup> laccase,<sup>24</sup> and palm tree peroxidase<sup>25</sup> possess remarkable advantages such as high substrate specificities and high efficiency under mild conditions. However, they also bear some serious shortages. For example, their catalytic activity can be easily inhibited and their preparation, purification and storage

are usually time-consuming and expensive. In order to conquer or decrease the influence of these shortages, more and more enzyme mimics including porphyrin,<sup>26</sup> hematin<sup>27</sup> and phthalocyanine<sup>28</sup> have been synthesized and applied to catalyze the polymerization of aniline. But these reported enzyme mimics are traditional organic substances which still show low stability in extreme conditions such as high temperature, strongly acidic/alkali, and whose fabrication is also complicated. Inorganic material show advantages to organic substances in better adaptation to extreme environment conditions and lower-cost fabrication, purification and storage. In 2007, Yan<sup>29</sup> prepared Fe<sub>3</sub>O<sub>4</sub> magnetic nanoparticles (Fe<sub>3</sub>O<sub>4</sub> MNPs) and found it's intrinsic peroxidase-like activity. Compared with HRP, the Fe<sub>3</sub>O<sub>4</sub> MNPs can keep a stable relative activity (standard conditions pH 3.5 and 40 °C) over a wide range of pH from 1 to 12, and temperature from 4 to 90 °C. In 2010, Song<sup>30</sup> found the peroxidase catalytic activity of graphene oxide (GO-COOH) which had even higher catalytic activity to tetramethylbenzidine (TMB) than HRP. Subsequently, carbon nanotubes,<sup>21</sup> Au nanoparticles,<sup>32</sup> CoFe<sub>2</sub>O<sub>4</sub> magnetic nanoparticles,<sup>33</sup> CePO<sub>4</sub> hollow spheres<sup>34</sup> and black elemental Se<sup>35</sup> were found to have peroxidase catalytic activity.

To date, very few reports concentrated on the green synthesis of PANI catalyzed by inorganic enzyme mimics are available. In this paper, we explored a green route to water-soluble PANI using iron phosphates (FePOs) peroxidase mimic reported by our group<sup>36</sup> to catalyze the polymerization of aniline. This method has the advantages of ordinary enzymatic method in that it is also eco-friendly and does not employ environmentally incompatible oxidant such as ammonium peroxydisulfate. Polymerization of aniline is initiated by H<sub>2</sub>O<sub>2</sub>, a naturally occurring mild oxidant and generally recognized as safe (GRAS) according to FDA. No other chemicals but H<sub>2</sub>O is generated as by-products. Superior to ordinary enzymatic method, this work used FePOs as a catalyst which is much cheaper and intrinsically more stable than natural enzymes against denaturation or protease digestion. Effects of reaction conditions on the conductivity of the prepared PANI were studied in details. The FePOs-catalyzed PANI was found to have a large light-to-heat conversion efficiency and can act as an efficient PTT agent to kill human cervical cancer (HeLa) cells.

## 40 Experimental

### Materials

All reagents used were of analytical quality. For the experiments, the following reagents were used: FeCl<sub>2</sub>·H<sub>2</sub>O, polyvinylpyrrolidone (PVP) and Na<sub>2</sub>HPO<sub>4</sub>·12H<sub>2</sub>O from Tianjin bodi chemical Co.,Ltd, NaH<sub>2</sub>PO<sub>2</sub>·H<sub>2</sub>O from ShangHai AiBi chemistry preparation Co.,Ltd, aniline (98%) from Alfa Aesar, sodium polystyrene sulfonate (PSS) from Shanghai Herochem Co.,Ltd., citric acid from Tianjin YongDa chemical reagent Co.,Ltd, glycol and hydrogen peroxide from Laiyang fine chemical factory.

### Synthesis of FePOs and green synthesis of water-soluble PANI catalyzed by FePOs

The preparation of FePOs was adopted from the method reported by our group.<sup>36</sup> Generally, 7 mmol of FeCl<sub>2</sub>·4H<sub>2</sub>O and 14 mmol of NaH<sub>2</sub>PO<sub>2</sub>·H<sub>2</sub>O were dissolved in 5 mL of distilled water, and

then mixed with 1 g of PVP dissolved in glycol (35 mL) under vigorous stirring to obtain a homogeneous solution. Afterwards the mixture was transferred into a 50 mL Teflon-lined autoclave, sealed and maintained at 180 °C for 24 h, then allowed to cool to the room temperature naturally. The resulting product was collected by centrifugation, washed with distilled water and ethanol for several times and finally dried in vacuum for 6 h.

In a typical polymerization reaction of PANI, to a 20 mL buffer solution (0.1 M citric acid and 0.2 M Na<sub>2</sub>HPO<sub>4</sub>) in a glass beaker, 0.6 mmol PSS was dispersed and stirred for 30 min in the ice bath. Then 0.6 mmol aniline monomer was added. After 10 h, 5 mg FePOs and 360–600 μL of 1 M H<sub>2</sub>O<sub>2</sub> solution were scattered into the solution and the polymerization was carried out for 24 h in a water bath kept at different temperature. The PANI solution was dialyzed in pH 5 HCl solution for 24 h using 8000~14000 molecular-weight cutoff dialysis bags twice to remove oligomers and unreacted monomer. Dry PANI samples were obtained by evaporation of final purified PANI solution and drying at 40 °C under vacuum for 24 h.

### 75 Measurement of conductivity of PANI

Purified PANI solution was coated onto two stainless steel sheets with a diameter of ~1.63 cm and thickness of ~0.082 cm. When the solution was about to dry up but still viscous, these two sheets were pressed together. After the sheets totally dried, the resistance of the PANI film was tested. Then the conductivity was calculated using the eq.1-2:

$$\rho = \frac{d}{RS} \quad \text{eq.1}$$

$$\sigma = \frac{1}{\rho} \quad \text{eq.2}$$

where  $d$  is the thickness of PANI film,  $R$  is the resistance of the PANI film,  $S$  is the surface area of stainless steel sheet,  $\rho$  is the resistivity of PANI film and  $\sigma$  is the conductivity of PANI film.

### Measurement of temperature rise and photothermal conversion efficiency of PANI

Dry PANI samples were dissolved in ultrapure water to obtain PANI solution with different concentrations (0–0.4 mg/mL). For the temperature rise of PANI solution, 808 nm NIR laser with an output of 1.0, 1.5 and 2.0 W was delivered through a 5 mL quartz cuvette containing PANI solution. The NIR laser was 20 cm away from the quartz cuvette. A digital thermometer with an accuracy of ±0.1 °C was inserted into the PANI solution perpendicular to the path of the laser. The temperature was recorded one time per 10 s for 10 min.

For the photothermal conversion efficiency of PANI, 2 mL PANI solution (0.2 mg/mL) was suspended in a 5 mL quartz cuvette. The NIR laser was 20 cm away from the quartz cuvette. The area of the light spot is 0.72 cm<sup>2</sup>. PANI solution was irradiated by 808 nm NIR laser at a power density of 2.08 W/cm<sup>2</sup> for 19 min (laser on), followed by naturally cooling to room temperature without NIR laser irradiation for 20 min (laser off). The temperature was recorded one time per 10 s using a digital thermometer with an accuracy of ±0.1 °C perpendicular to the path of the laser. The

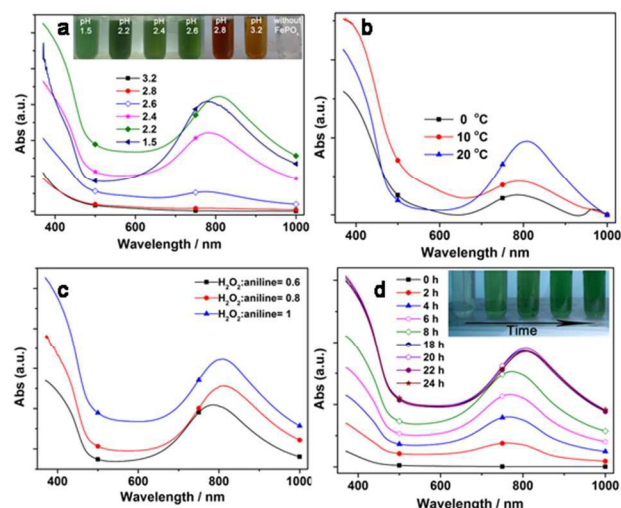


Fig.1 UV-Vis spectra of PANI synthesized at (a) different pH, the other synthetic conditions are 20 °C, 24 h, and the initial H<sub>2</sub>O<sub>2</sub>:aniline is 1.0; (b) different temperature, and the other synthetic conditions are 24 h, pH 2.2, H<sub>2</sub>O<sub>2</sub>:aniline=1.0; (c) different molar ratios of H<sub>2</sub>O<sub>2</sub>/aniline, and the other synthetic conditions are 24 h, pH 2.2, 20 °C; (d) different time, and the other synthetic conditions are pH 2.2, H<sub>2</sub>O<sub>2</sub>:aniline=1.0, 20 °C. The insets are the images of PANI solution synthesized with (a) different pH value, (d) different time.

photothermal efficiency,  $\eta$ , was calculated using the following eq.3-4.<sup>8,13</sup>

$$\eta = \frac{hS(T_{\max} - T_{\text{surr}}) - Q_{\text{dis}}}{I(1 - 10^{-A_{808}})} \quad \text{eq.3}$$

$$hS = \frac{Cm}{\tau_s} \quad \text{eq.4}$$

where  $h$  is heat transfer coefficient,  $S$  is the surface area of the container.  $T_{\max}$  is the equilibrium temperature, and  $T_{\text{surr}}$  is ambient temperature of the surroundings.  $Q_{\text{dis}}$  represents heat dissipated from light absorbed by the quartz sample cell itself, and it was calculated independently using a quartz sample cell containing ultrapure water without PANI.  $I$  is incident laser power density.  $A_{808}$  is the absorbance intensity of the prepared PANI at 808 nm. Time constant ( $\tau_s$ ) for heat transfer from the system is determined as the slop by applying the linear time data from the cooling period *versus* negative natural logarithm of driving force temperature.  $C$  is the heat capacity of water.  $m$  is the mass of PANI solution.

### Cell culture and photothermal therapy

Cell viability of FePOs-catalyzed PANI was accessed by a colorimetric measure, based on the mitochondrial oxidation of 3-(4,5-dimethylthiazolyl-2)-2,5-diphenyltetrazolium bromide (MTT). HeLa cells were harvested at a density of  $5 \times 10^3$  per well in a 96-cell plate with DMEM medium containing 10% calf serum and incubated at 37 °C under a 5% CO<sub>2</sub>. Subsequently, the cells were incubated with different concentrations of PANI diluted with DMEM medium for 24 h. Afterwards, the medium was removed and the cells were treated with freshly prepared 20

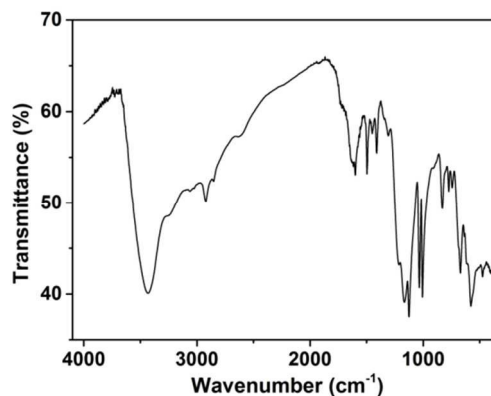


Fig.2 FTIR spectrum of PANI synthesized at 20 °C in pH 2.2 buffer solution for 20 h with H<sub>2</sub>O<sub>2</sub>:aniline=1.0.

$\mu\text{L}$  MTT solution (5 mg/mL MTT in phosphate buffer solution (PBS), pH 7.4) and incubated for another 4 h before adding 100  $\mu\text{L}$  of dimethyl sulfoxide. The plate was oscillated for 10 min at 37 °C, then the absorbance of each well at 490 nm was measured on a microplate reader.

For photothermal cancer cell killing, HeLa cells were incubated with 0.4 mg/mL PANI in 24-well plate with DMEM medium at 37 °C for 24 h. Afterwards, the medium was removed and 100  $\mu\text{L}$  fresh DMEM medium was added into each well. Then HeLa cells were irradiated by 808 nm laser with an output of 0.8 or 1.0 W for 10 min and stained by trypan blue solution (0.4 wt%). Microscopic images of cells were then taken using an inverted microscope.

### Characterization of PANI

UV-Vis detection was carried out using a Cary 500 UV-Vis-NIR spectrophotometer (Varian, USA). FTIR spectrum was achieved with a VERTEX70 Fourier transform infrared spectrometer (Bruker, German). The absorbance of each well at 490 nm was measured on a microplate reader (Bio-RAD Model 680). Photothermal therapy experiment was carried out using a continuous-wave diode NIR laser (Xi'an Minghui Optoelectronic Technology, China) with a center wavelength of  $808 \pm 10$  nm. An inverted microscope (Eclipse TE2000S, Nikon) was used to image the HeLa cells.

### Results and discussion

The FePOs, prepared in the way reported by Wei Wang et al,<sup>36</sup> has intrinsic peroxidase-like activity. Inspired by this activity, the FePOs is applied to catalyze the green synthesis of water-soluble PANI using PSS as template. First of all, we tentatively tested the catalytic ability of FePOs. As shown in the inset of Fig.1a, the color of the reaction system (pH=2.2) without FePOs shows no obvious change. But those catalyzed by FePOs presented apparent color change at different pH values. So the FePOs indeed can catalyze the polymerization of aniline as the natural enzyme do. Also the picture demonstrated good water-solubility of PANI.

UV-Vis spectra (Fig.1) indicate that all samples showed typical absorption band of PANI around 800 nm. Fig.2 is the FTIR spectrum (on KBr) of the samples. The broad absorption peak



centered at  $3432\text{ cm}^{-1}$  corresponds to the  $-\text{NH}_2$  asymmetric stretching. The peak at  $1600\text{ cm}^{-1}$  corresponds to  $\text{N}=\text{Q}=\text{N}$  stretching. The peak around  $1496\text{ cm}^{-1}$  can be attributed to  $\text{N}-\text{B}-\text{N}$  stretching (B, benzenoid unit). The peaks at  $1450$  and  $1411\text{ cm}^{-1}$  are assigned to stretching of benzene ring and  $\text{C}-\text{N}$  stretching in QBQ units (B, benzenoid unit; q, quinonoid unit),<sup>35</sup> respectively. The  $\text{C}-\text{H}$  out-of-plane bending of 1,4-ring can be found at  $\sim 830\text{ cm}^{-1}$ , indicating that aniline polymerized through head-to-tail.<sup>38</sup> The peaks observed at  $1006$  and  $1034\text{ cm}^{-1}$  correspond to symmetric and asymmetric  $\text{S}=\text{O}$  stretching, and a band at  $670\text{ cm}^{-1}$  which is attributed to the  $-\text{SO}_3$  group further confirms the presence of PSS in the complex.<sup>39</sup> All the information above suggest that the product we synthesized is the complex of PSS and PANI.

In order to study the effect of synthetic conditions, polymerization of PANI was carried out at different pH and temperatures with different molar ratios of  $\text{H}_2\text{O}_2$ :aniline and reaction time. UV-Vis spectra of PANI synthesized at different conditions (Fig.1) exhibit two sets of absorption peak. One is a shoulder observed at  $\sim 430\text{ nm}$  which corresponds to an intermediate redox state of PANI, another one is a broad band centered at  $\sim 800\text{ nm}$  which is ascribed to the emeraldine state of PANI<sup>40-42</sup> and compared as a signature of the formation of conductive PANI due to polaron band transitions.<sup>4,41</sup>

The UV-Vis spectra of PANI synthesized at the pH range of 1.5–3.2 are given in Fig.1a. Observation of the intensity of the polaron band at  $800\text{ nm}$  suggests that the extent of polymerization was highest at pH 2.2 (maximum intensity) and least at pH 3.2 (minimum intensity) during the same time period. When the pH value increased from 1.5 to 2.6, the conductivity of PANI reached the highest ( $2.576 \times 10^{-3}\text{ S/cm}$ ) at pH 2.2 and the lowest ( $0.393 \times 10^{-3}\text{ S/cm}$ ) at pH 2.6 (Table 1). As the pH value further increased, the green PANI was altered to yellow (inset of Fig.1a) corresponding to the disappearance of the polaron band at  $800\text{ nm}$  in the UV-Vis spectra. These results thus showed that the FePOs-catalyzed polymerization of PANI was strongly pH-dependent. Wherein the optimal pH (2.2) was needed to provide the highest conductivity and highest absorbance at  $800\text{ nm}$  of emeraldine form of PANI.

Table.1 Conductivity of PANI formed at different condition

		Conductivity ( $\times 10^{-3}\text{ S/cm}$ )
pH 20 °C	1.5	1.857
	2.2	2.576
	2.4	1.285
	2.6	0.393
Temperature (°C) (pH=2.2)	0	0.263
	10	0.367
	20	2.576
Molar ratio of $\text{H}_2\text{O}_2$ and aniline (pH=2.2, 20 °C)	0.6	0.127
	0.8	0.136
	1.0	2.576

It is well-known that most natural enzymes are active in near neutral pH conditions. For example, the optimal pH for the catalytic activity of HRP is about pH 6.0. Samuelson<sup>43</sup> reported that at room temperature this activity decreased as the pH is lowered in PSS solutions and quickly dropped to only 20% of the original activity at pH 4.0 after 20 min, dropping to near zero activity at longer times. Unfortunately, PSS is a strongly acidic polyelectrolyte and can play the template role only at pH lower

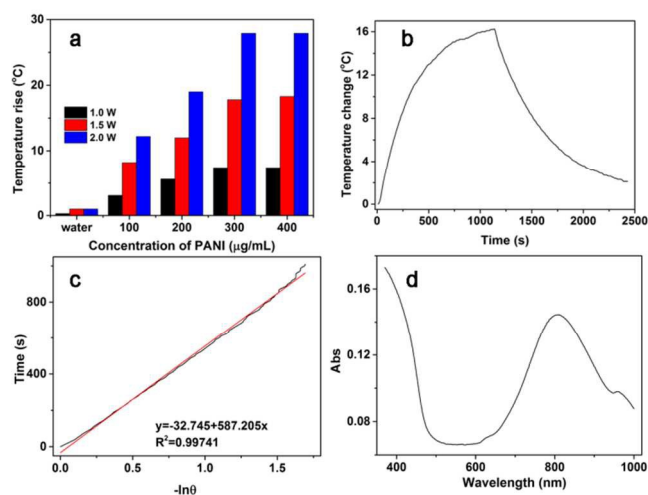


Fig.3 (a) The temperature rise of 2 mL PANI solution with various concentrations under 808 nm laser irradiation. (b) Photothermal effect of the irradiation of the PANI solution with the NIR laser (808 nm,  $2.08\text{ W/cm}^2$ ), in which the irradiation lasted for 19 min, and then the laser was shut off. (c) Linear calibration plot between time and negative natural logarithm of driving force temperature, which is obtained from the cooling stage of panel b. Time constant for heat transfer from the system is determined to be  $\tau_s = 587.205\text{ s}$ . (d) UV-Vis spectrum of PANI synthesized in pH 2.2 buffer solution at  $20\text{ °C}$  for 20 h.

than 4.65. As a result, the pH had to be strictly limited between 4.3–4.65 to ensure both adequate activity of the enzyme and electrostatic interaction to form the emeraldine salt of polyaniline.

From Fig.1a, it is clear to see that the signature band of conductive PANI at  $600\text{--}1000\text{ nm}$  are still very strong even at a very low pH of 1.5. The green color of the resulting PANI solutions obtained at pH 1.5 (in set of Fig.1a) further confirms the formation of water soluble conductive PANI. Consequently, compared with natural enzymes our FePOs peroxidase mimic demonstrates robustness by the ability to catalyze the conductive PANI-PSS synthesis at much lower pH values, indicating a distinct advantage over natural enzymes.

The effects of temperature on the UV-Vis absorbance and conductivity of PANI were shown in Fig.1b and the second line of Table.1, respectively. From Fig.1b, one can see the typical absorption peak corresponding to the emeraldine state of PANI at  $\sim 800\text{ nm}$ .<sup>40-42</sup> This peak showed an enhancement and a slightly red shift from  $\sim 790\text{ nm}$  ( $0\text{ °C}$ ) to  $\sim 805\text{ nm}$  ( $20\text{ °C}$ ) as the temperature increased. It is well known that the UV-Vis absorbance band shifts longer wavelengths with a longer conjugated molecular chain.<sup>44-45</sup> Thus, the PANI formed at  $20\text{ °C}$  had longer conjugated chain. As the temperature rised from  $0\text{ °C}$  to  $20\text{ °C}$ , conductivity of PANI increased from  $0.263 \times 10^{-3}\text{ S/cm}$  to  $2.576 \times 10^{-3}\text{ S/cm}$ . Therefore we chosed  $20\text{ °C}$  to synthesize PANI.

As demonstrated by Fig.1c, when the molar ratio of  $\text{H}_2\text{O}_2$  and aniline ( $\text{H}_2\text{O}_2$ :aniline) was 1.0, PANI showed strongest absorbance at  $\sim 800\text{ nm}$ . This result was in consistent with the conductivity measurement as shown in Table.1, in which the conductivity of PANI increased with  $\text{H}_2\text{O}_2$ :aniline and reached the highest value of  $2.576 \times 10^{-3}\text{ S/cm}$  when  $\text{H}_2\text{O}_2$ :aniline was 1.0. So we confirm that the optimal molar ratio of  $\text{H}_2\text{O}_2$  and aniline

was 1.0.

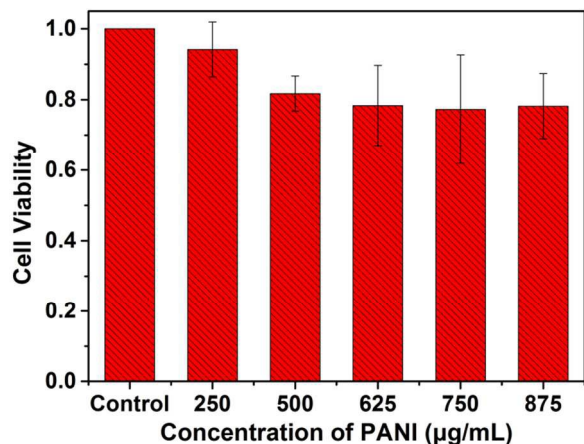


Fig.4 Cell viability of HeLa cells after being incubated with various concentrations of FePO<sub>4</sub>-catalyzed PANI for 24 h. Data presented as mean ±SD ( $n = 12$ ). \* $p < 0.05$  when compared with control.

In Fig.1d, one can see that the intensity of the signature band increased as the reaction proceeded. Accordingly, the green color characteristic of conducting PANI gradually developed (inset of Fig.1d), indicating an increase in molecular weight of the polymer with time since the absorption of the polaron band is strongly dependent on the molecular weight and protonation level of PANI.<sup>4</sup> After 20 h, the absorbance didn't show further increase. Therefore the optimal reaction time was 20 h.

To investigate the hyperthermic potential of PANI, we evaluated photothermal effect generated by PANI with the conductivity of  $2.576 \times 10^{-3}$  S/cm upon NIR laser irradiation. Being irradiated by a 808 nm laser light (2.0 W) for 10 min, a remarkable temperature increase of 12.2~27.9 °C was observed for 2 mL of the prepared PANI (with a 5 mL quartz sample cell) with concentrations ranging from 0.1 to 0.4 mg/mL (blue columns in Fig.3a). Smaller temperature rise of 8.2~18.3 °C (red columns in Fig.3a) and 3.1~7.4 °C (black columns in Fig.3a) were observed for the lower laser power of 1.5 and 1.0 W, respectively. The temperature increase of pure water is 0.3~1.0 °C under 1.0~2.0 W laser light irradiation, which is much lower than that observed for the prepared PANI, further indicating the photothermal effect of our FePO<sub>4</sub> catalyzed PANI.

Fig.3b shows the typical thermal profile of the PANI solution. Time constant ( $\tau_s$ ) for heat transfer from the system can be determined to be 587.205 s by the slope of the fitted line shown in Fig.3c. The value of  $hS$  was calculated to be 14.26 mW/°C using eq.4. ( $T_{\max} - T_{\text{surr}}$ ) was 16.3 °C according to Fig.3b. The  $Q_{\text{dis}}$  was calculated to be 10.78 mW.  $I$  is incident laser power density (2.08 W/cm<sup>2</sup>).  $A_{808}$  was measured to be 0.144 from Fig.3d. Thus, the 808 nm laser light-to-heat conversion efficiency ( $\eta$ ) of the prepared PANI (pH 2.2, 20 °C, 20 h) can be calculated to be 39.6% by eq.3. This value is lower than that of F127 (ethylene oxide/propylene oxide block copolymer)-modified PANI nanoparticles (48.5%) as reported by Zhou et al.<sup>16</sup> The lower efficiency of our product can be ascribed to the presence of PSS without photothermal effect but with a high theoretical mass percentage of 68.9% in the PANI-PSS complex. Nevertheless, our PANI still has advantages in its water-solubility which is

desirable for practical applications, especially for bio-applications.

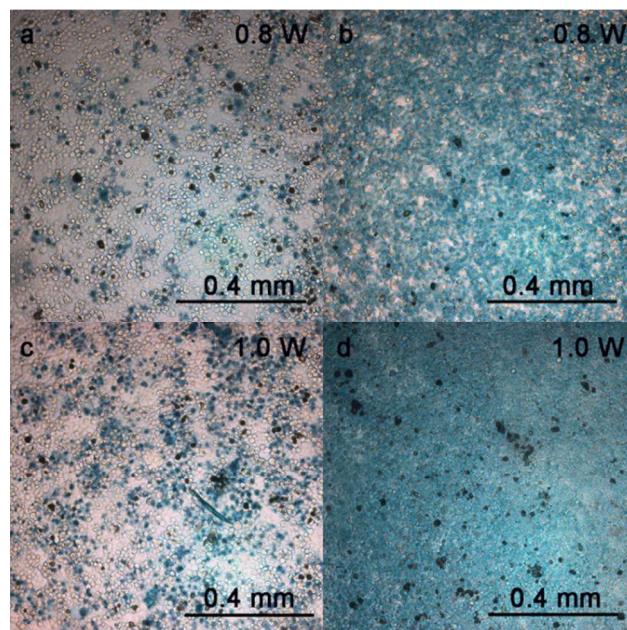


Fig.5 Optical microscopic images of HeLa cells incubated (a, c) without PANI, (b, d) with PANI (0.4 mg/mL), which were irradiated by 808 nm laser for 10 minutes and then stained by trypan blue.

In contrast, PANI nanoparticles prepared by Zhou et al without modification were not easily dispersed in water as the authors described. F127 was used to enhance the water dispersity of PANI nanoparticles, which complicated the fabrication of PANI photothermal agent.

For the application of PANI in PTT, firstly we investigated its biocompatibility. Fig.4 shows the cell viability data of HeLa cells incubated with different concentrations of PANI sample that has a light-to-heat conversion efficiency ( $\eta$ ) of 39.6%. The final results were expressed as the average of six parallel experiments ± the standard deviations (denoted as error). As the figure provided, the percentage of viable cells was  $(94.2 \pm 7.7)\%$  after 24 h incubation with PANI with the concentration as high as 0.25 mg/mL. No significant inhibition of growth and proliferation was observed up to a 0.875 mg/mL concentration of PANI. Consequently, the as-prepared PANI appears to be largely biocompatible.

HeLa cell was used as a cell model to investigate the anti-tumor effect of the prepared PANI via PTT mechanism. The concentration of PANI for in vitro PTT test was determined to be 0.4 mg/mL to ensure adequate heat efficiency as well as low toxicity of PANI. HeLa cells were incubated with the PANI (0.4 mg/mL) for 24 h and then irradiated by 808 nm laser light (0.8 W) for 10 min. After that the cells were stained by TB for 10 min, which can detect the integrity of the cell membrane, in order to differentiate the dead and live cells. As shown in Fig.5b and Fig.5d, lots of cells incubated with PANI were stained blue, demonstrating a high cell death rate after irradiation of 808 nm laser with light power of 0.8 W or 1.0 W for 10 minutes. Whereas few cells were stained blue for those incubated without PANI but merely irradiated by 808 nm laser with the same power for 10



minutes (Fig.5a and Fig.5c). Compared with Fig.5b, much more cells were observed to be blue (Fig.5d), suggesting an enhanced cell-killing effect due to increased light power. The remarkable disparity in cell death rates between the cells incubated with and without PANI demonstrates potential applications of the FePOs catalyzed PANI as an efficient PTT agent.

## Conclusions

In conclusion, by using FePOs peroxidase mimic as a catalyst, we synthesized water-soluble PANI in environmentally mild conditions as natural enzymes do. The advantage of the prepared FePOs peroxidase mimic over natural peroxidase lies with its robust catalytic ability at much lower pH values. The optimal polymerization conditions are pH 2.2, 20 °C and the molar ratio of H<sub>2</sub>O<sub>2</sub>:aniline = 1.0. PANI formed in these conditions showed the highest conductivity of  $\sim 2.576 \times 10^{-3}$  S/cm and a satisfied photothermal conversion efficiency of 39.6% after exposure to 808 nm laser light (2.08 W/cm<sup>2</sup>) irradiation. The in vitro experiment on HeLa cells proved the as-prepared PANI has good biocompatibility. Remarkable tumor cells killing effect via PTT mechanism suggests that the as-prepared PANI can be a good candidate as a photothermal agent.

## Acknowledgements

This research was financially supported by Distinguished Middle-Aged and Young Scientist Encourage and Reward Foundation of Shandong Province (Grant No. BS2012CL015) and Development Program in Science and Technology of Qingdao (Grant No. 13-1-4-182-jch).

## Notes and references

- <sup>a</sup> Lab of Functional and Biomedical Nanomaterials, College of Materials Science and Engineering, Qingdao University of Science and Technology, Qingdao, 266042 (China) Fax: 86 532 84022509; E-mail: wangwei@qust.edu.cn; kchen@qust.edu.cn
- <sup>b</sup> Yebio Bioengineering Co. Ltd, Qingdao, 266032 (China)
- \* To whom correspondence should be addressed.
- J. W. Xiao, S. X. Fan, F. Wang, L. D. Sun, X. Y. Zheng and C. H. Yan, *Nanoscale*, 2014, **6**, 4345.
  - X. Huang, P. K. Jain, I. H. El-Sayed and M. A. El-Sayed, *Lasers med. Sci.*, 2008, **23**, 217.
  - W. Wu, J. Shen, P. Banerjee and S. Zhou, *Biomaterials*, 2011, **32**, 598.
  - W. Wu, J. Shen, P. Banerjee and S. Zhou, *Biomaterials*, 2010, **31**, 7555.
  - H. Kang, A. C. Trondoli, G. Zhu, Y. Chen, Y. J. Chang, H. Liu, Y. F. Huang, X. Zhang and W. Tan, *ACS Nano*, 2011, **5**, 5094.
  - P. K. Jain, I. H. El-Sayed and M. A. El-Sayed, *Nano Today*, 2007, **2**, 18.
  - W. I. Choi, J. Y. Kim, C. Kang, C. C. Byeon, Y. H. Kim and G. Tae, *ACS Nano*, 2011, **5**, 1995.
  - J. Li, J. Han, T. Xu, C. R. Guo, X. Y. Bu, H. Zhang, L. P. Wang, H. C. Sun and B. Yang, *Langmuir*, 2013, **29**, 7102.
  - S. Tang, X. Huang and N. Zheng, *Chem. Commun.*, 2011, **47**, 3948.
  - X. Huang, S. Tang, B. Liu, B. Ren and N. Zheng, *Adv. Mater.*, 2011, **23**, 3420.
  - T. N. Lambert, N. L. Andrews, H. Gerung, T. J. Boyle, J. M. Oliver, B. M. Wilson and S. M. Han, *Small*, 2007, **3**, 691.
  - N. W. S. Kam, M. O'Connell, J. A. Wisdom and H. J. Dai, *Proc. Natl. Acad. Sci. U. S. A.*, 2005, **102**, 11600.
  - Q. Tian, F. Jiang, R. Zou, Q. Liu, Z. Chen, M. Zhu, S. Yang, J. Wang, J. Wang and J. Hu, *ACS Nano*, 2011, **5**, 9761.

- S. Link, C. Burda, M. B. Mohamed, B. Nikoobakht and M. A. El-Sayed, *J. Phys. Chem. A*, 1999, **103**, 1165.
- S. Link, C. Burda, B. Nikoobakht and M. A. El-Sayed, *J. Phys. Chem. B*, 2000, **104**, 6152.
- J. Zhou, Z. Lu, X. Zhu, X. Wang, Y. Liao, Z. Ma and F. Li, *Biomaterials*, 2013, **34**, 9584.
- Z. Zha, X. Yue, Q. Ren and Z. Dai, *Adv. Mater.*, 2013, **25**, 777.
- K. M. Au, M. Chen, S. P. Armes and N. F. Zheng, *Chem. Commun.*, 2013, **49**, 10525.
- C. M. MacNeill, R. C. Coffin, D. L. Carroll and N. H. Levi-Polyachenko, *Macromol. Biosci.*, 2013, **13**, 28.
- J. Yang, J. Choi, D. Bang, E. Kim, E. K. Lim, H. Park, J. S. Suh, K. Lee, K. H. Yoo, E. K. Kim, Y. M. Huh and S. Haam, *Angew. Chem. Int. Ed.*, 2011, **50**, 441.
- C. W. Hsiao, H. L. Chen, Z. X. Liao, R. Sureshbabu, H. C. Hsiao, S. J. Lin, Y. Chang and H. W. Sung, *Adv. Funct. Mater.*, 2014, DOI: 10.1002/adfm.201403478.
- A. J. Heeger, *Angew. Chem. Int. Ed.*, 2001, **40**, 2591.
- L. A. Samuelson, A. Anagnostopoulos, K. S. Alva, K. Senecal, J. Kumar, S. Tripathy and L. Samuelson, *Macromolecules*, 1998, **31**, 4376.
- A. V. Karamyshev, S. V. Shleev, O. V. Koroleva, A. I. Yaropolov and I. Y. Sakharov, *Enzyme Microb. Technol.*, 2003, **33**, 556.
- I. Y. Sakharov, A. C. Vorobiev and J. J. C. Leon, *Enzyme Microb. Technol.*, 2003, **33**, 661.
- M. R. Nabid, R. Sedghi, P. R. Jamaat, N. Safari and A. A. Entezami, *J. Appl. Polym. Sci.*, 2006, **102**, 2929.
- S. Roy, J. M. Fortier, R. Nagarajan, S. Tripathy, J. Kumar, L. A. Samuelson and F. F. Bruno, *Biomacromolecules*, 2002, **3**, 937.
- M. R. Nabid, R. Sedghi, P. R. Jamaat, N. Safari and A. A. Entezami, *Appl. Catal., A: General*, 2007, **328**, 52.
- L. Gao, J. Zhuang, L. Nie, J. B. Zhang, Y. Zhang, N. Gu, T. H. Wang, J. Feng, D. L. Yang, S. Perrett and X. Y. Yan, *Nature Nanotech.*, 2007, **2**, 577.
- Y. Song, K. Qu, C. Zhao, J. Ren and X. Qu, *Adv. Mater.*, 2010, **22**, 2206.
- R. Cui, Z. Han and J. J. Zhu, *Chem. Eur. J.*, 2011, **17**, 9377.
- Y. Jv, B. Li and R. Cao, *Chem. Commun.*, 2010, **46**, 8017.
- W. Shi, X. Zhang, S. He, S. H. He and Y. M. Huang, *Chem. Commun.*, 2011, **47**, 10785.
- W. Wang, X. P. Jiang and K. Z. Chen, *Chem. Commun.*, 2012, **48**, 6839.
- L. L. Li, W. Wang and K. Z. Chen, *J. Phys. Chem. C*, 2014, **118**, 26351.
- W. Wang, X. P. Jiang and K. Z. Chen, *Chem. Commun.*, 2012, **48**, 7289.
- E. T. Kang, K. G. Neoh and K. L. Tan, *Prog. Polym. Sci.*, 1998, **23**, 277.
- Y. Furukawa, F. Ueda, Y. Hyodo, I. Harada, T. Nakajima and T. Kawagoe, *Macromolecules*, 1988, **21**, 1297.
- M. R. Nabid and A. A. Entezami, *J. Appl. Polym. Sci.*, 2004, **94**, 254.
- G. D'Aprano, M. Leclerc and G. Zotti, *J. Electroanal. Chem.*, 1993, **351**, 145.
- M. Scully, M. C. Petty and A. P. Monkman, *Synth. Met.*, 1993, **55**, 183.
- M. Kirschenmann, D. Wöhrle and W. Vielstich, *Ber. Bunsen Ges. Phys. Chem.*, 1988, **92**, 1403.
- W. Liu, J. Kumar, S. Tripathy, K. J. Senecal and L. Samuelson, *J. Am. Chem. Soc.*, 1999, **121**, 71.
- J. L. Brédas and G. B. Street, *Acc. Chem. Res.*, 1985, **18**, 309.
- J. L. Brédas, J. C. Scott, K. Yakushi and G. B. Street, *Phys. Rev. B: Condens. Matter*, 1984, **30**, 1023.